Vol 18 No 4, April 2009
1674-1056/2009/18(04)/1609-05

Chinese Physics B

© 2009 Chin. Phys. Soc.
and IOP Publishing Ltd

Localized states of flattened quantum elliptic rings and their optical properties*

Situ Shu-Ping(司徒树平)†

Department of Physics, Sun Yat-Sen University, Guangzhou 510275, *China*

(Received 22 March 2008; revised manuscript received 10 November 2008)

A flattened elliptic ring containing an electron is studied. The emphasis is placed on clarifying the effect of the flattening. The localized states are classified into four types according to their inherent nodes. When the ring becomes more flattened, the total probability of dipole absorption of each state is found to be reduced. Furthermore, each spectral line of absorption is found to shift towards red and may split into a few lines, and these lines as a whole become more diffusive.

Keywords: flattened quantum elliptic ring, localized state, dipole absorption
PACC: 7320D, 7800

It is recognized that micro-devices are important for micro-techniques. Various kinds of micro-devices, including the quantum rings,[1,2] have been extensively studied theoretically and experimentally in recent years. Quantum rings are different from other devices due to their special geometry. A well-known phenomenon of the ring is the Aharonov–Bohm oscillation of the ground state energy and persistent current.[3−6] It is believed that the ring geometry would effectively affect the properties of small systems. Therefore, in addition to circular rings, elliptic rings or rings with other specific geometries deserve to be studied, because new and special properties might be found. There has been a vast literature devoted to elliptic quantum dots,[7−10] but not so much literature dealing with elliptic rings. The present paper is devoted to the latter as a complement to the study in this respect.

We consider an electron with an effective mass m^* strictly confined in an X–Y plane in a region between two ellipses having the same focuses, and beyond this region we assume wavefunctions to be zero. Such a case of strong confinement has been considered by Berman *et al.*[11] They found the appearance of the confined states free from the Aharonov–Bohm oscillations, and these states were expected to exist commonly in the systems with broken symmetry.[7] However, in their studies, the optical property was not studied. In the present paper the result in Ref.[11] is generalized by using a slightly different method and a detailed analysis of the confined states is also made. In particular, since the optical property is generally useful for some applications, the feature of the absorption spectrum of radiation is studied in the present paper. The emphasis is placed on demonstrating the effect of the flattening of the ring, therefore different degrees of flattening are considered.

Let the inner and the outer ellipses of the boundary of the region have half major axes $r_{\rm a}$ and $r_{\rm b}$, respectively, and both ellipses have identical focuses with the focal distance R. Introduce the elliptical coordinates λ and μ, then we will have $x = R\lambda\mu/2$, and $y = \pm R\sqrt{(\lambda^2-1)(1-\mu^2)}/2$. Therefore, the Hamiltonian of the one-electron system reads[12]

$$H = 4G/(\lambda^2-\mu^2)\bigg[-(\lambda^2-1)\frac{{\rm d}^2}{{\rm d}\lambda^2} - 2\lambda\frac{\rm d}{{\rm d}\lambda} -(1-\mu^2)\frac{{\rm d}^2}{{\rm d}\mu^2} + 2\mu\frac{\rm d}{{\rm d}\mu}\bigg], \quad (1)$$

where $G = \hbar^2/(2m^*R^2)$. In the present paper, an external magnetic field is not considered, and its effect will be studied elsewhere. It is recalled that λ is a constant for an ellipse, specifically, the inner ellipse has $\lambda_{\rm in} = 2r_{\rm a}/R$, while the outer ellipse has $\lambda_{\rm out} = 2r_{\rm b}/R$. Thus, the elliptical ring extends from $\lambda_{\rm in}$ to $\lambda_{\rm out}$, while μ extends from –1 to 1. For the convenience of calculation, introduce two parameters, i.e. $\lambda_0 = (\lambda_{\rm in} + \lambda_{\rm out})/2$ and $d_\lambda = \lambda_{\rm out} - \lambda_{\rm in}$, and then define $t = \pi(\lambda - \lambda_0)/d_\lambda$ and $\theta = \cos^{-1}\mu$. In

*Project supported by the National Natural Science Foundation of China (Grant Nos 10574163 and 10675174).
†E-mail: stsstsp@mail.sysu.edu.cn

other words, we have changed the arguments from λ and μ into t and θ respectively, where t ranges from $-\pi/2$ to $\pi/2$, and θ from 0 to 2π. With the new arguments, we introduce two sets of basis functions, namely, $f_m(t) = \cos mt$ (m is an odd positive integer) and $f_m(\mathrm{t}) = \sin m't$ (m' is an even positive integer), and $\mathrm{e}^{\mathrm{i}k\theta}$ (k is an integer ranging from $-k_{\max}$ to $k_{\max}$). Then diagonalizing the Hamiltonian yields the eigenenergy E_i of the i-th state $\Psi_i = \sum_{m,k} c_{m,k} f_m(t)\mathrm{e}^{\mathrm{i}k\theta}$. Using Ψ_i, we can calculate the current circulating around the elliptical ring† as

$$J_i = \frac{\hbar}{2m^*} \int \left[\Psi_i^* \left(-\mathrm{i}\frac{\mathrm{d}}{\mathrm{d}\theta} \right) \Psi_i + \mathrm{c.c.} \right] \frac{\mathrm{d}\lambda}{\sqrt{\lambda^2 - 1}}. \quad (2)$$

We can also calculate the probability of the dipole transition from initial state Ψ_i to final state Ψ_f as

$$P_{\mathrm{f},i} = \frac{2}{3} \left(\frac{\omega}{c} \right)^3 \frac{e^2}{\hbar} \times \left| \left\langle \Psi_\mathrm{f} \left| \frac{R}{2} (\lambda \cos\theta \pm \mathrm{i}\sqrt{\lambda^2 - 1} \sin\theta) \right| \Psi_i \right\rangle \right|^2, \quad (3)$$

where $\hbar\omega$ is the photon energy.

In what follows nm and meV are used as units of length and energy, the parameters are taken as $m^* = 0.063\, m_\mathrm{e}$ (for InGaAs rings), $r_\mathrm{a} = 100$, $r_\mathrm{b} = 150$ and the values of R are given in three cases, i.e. $R = 0.001$ (very close to a circle), 20, and 40 to show the effect of the flattening of the ring. The results and analysis are presented as follows.

Let $R = 0.001$, 20, and 40 be denoted by cases (A), (B), and (C), respectively. The ground state energies for these three cases are 2.378, 2.369, and 2.342, respectively, i.e. the energy of the more flattened ring is lower. The spectra of these three cases are given in Fig.1, where all the ground state energies are rescaled to zero. It is surprisingly found that the upper parts of the three spectra are very similar, but the lower parts are different. For examples, E_2 and E_3 are degenerate in case (A), but they split in case (B), and the splitting becomes larger in case (C). These spectra demonstrate that the lower states can be seriously affected by the flattening.

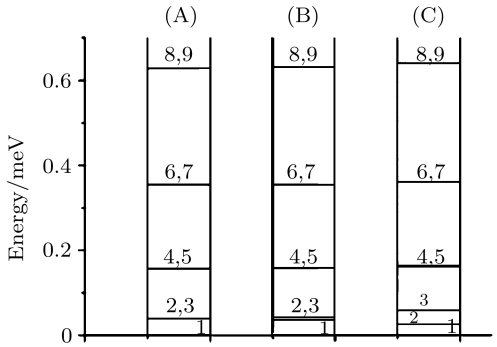


Fig.1. Low-lying spectra of three cases $R = 0.001$ (A), 20 (B), and 40 nm (C) where the ground state energies of these three cases are 2.378, 2.369 and 2.342 meV respectively and all the ground state energies are rescaled to zero.

The currents J_i/c of the Ψ_i states with $i = 1$ to 36 are plotted in Fig.2(a). The three i-th states in the three cases have similar currents in magnitude if i is larger, just as they have similar energies as shown in Fig.1. However, if i is small, the currents for cases (B) and (C) are zero. For example, for case (B), the states $\Psi_1 - \Psi_5$ have zero current, which is clearly indicated in Fig.2(b). Starting from Ψ_6, the currents increase suddenly with magnitude increasing, which is similar to the behaviour of corresponding states of the circular ring (case (A)). The zero current is a strong signal whose corresponding states $\Psi_1 - \Psi_5$ are localized states (or confined states), which supports the findings given in Refs.[7, 11]. Furthermore, from Fig.2 the following points can be found.

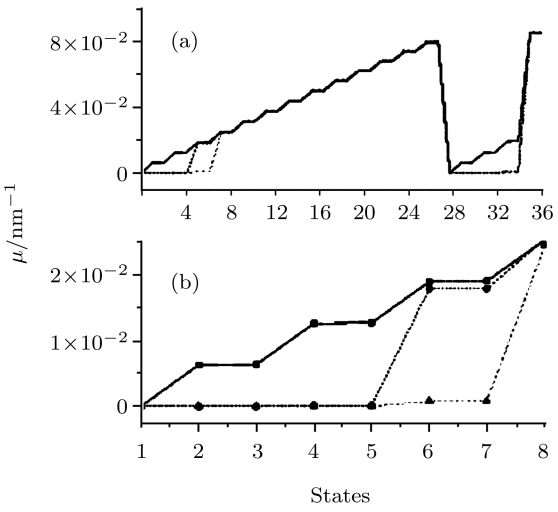


Fig.2. Currents $|J_i|/c$ of Ψ_i states 1 to 36, where solid, dash, and dot lines are for the cases (A), (B), and (C) respectively and panel (b) shows the magnification of the left-down corner of panel (a).

† Expression (2) is acquired via the following steps. The first step is to obtain the components of the current along x and y axes from the conservation law that is well known. The second step is to obtain the component along the tangent of an ellipse j_θ. The last step is to integrate j_θ along λ from λ_in to λ_out, and then expression (2) is obtained.

(i) A more flattened ring has more localized states. For example, if the values of R are 0.001, 20 and 40, the numbers of localized states are 1, 5 and 7, respectively. We have further calculate the case where $R = 80$, and 11 localized states are found.

(ii) The localized states appear not only in the lower part of spectra, but also in the upper part. In fact, there are two types of excitations, namely, circular excitation related to θ, and radial excitation related to λ. The low-lying spectrum is dominated by the circular excitation, where the electron in a higher state can rotate faster, thereby giving rise to a stronger current. However, state 28 does not experience any circular excitation (its current is zero as shown in Fig.2(a)): it is excited purely by radial excitation. In fact, it initiates an excited rotation band characterized by a quantum of radial excitation as compared with the ground band initiated by the ground state ($i = 1$). From Fig.2(a) we know that states 28–34 belong to the excited band. When $i \geq 35$, the members of the two bands will appear alternatively. Higher rotation bands will also appear when the energy goes higher and higher. It is noted that, for each rotation band, the first a few members become localized states if the ring becomes flattened. For examples, for case (C), the states 1–7 and 28–34 are localized as shown in Fig.2(a).

Then the structures of the low-lying states are investigated. For case (C), at $t = 0$ when $\lambda = \lambda_0$, Ψ_i as a function of θ is plotted in Fig.3. States 1, 3, 5, and 7 in Fig.3(a) and states 2, 4, and 6 in Fig.3(b) are all localized states while state 12 in Fig.3(c) is a non-localized (or extended) state that is plotted here for a comparison. The wavefunctions of all the localized states are real. For the ground state, the distribution is more concentrated in the neighbourhoods of $\theta = \pi/2$ and $3\pi/2$, i.e. in the upper part and the lower part of the flattened ring. This state is symmetric with respect to $\theta \to -\theta$ (up-down symmetry) and is also symmetric with respect to $\theta \to \pi - \theta$ (left-right symmetry). In general, we find that the localized states can be classified into four types. Type I is both up-down and left-right symmetric (e.g. states 1 and 5). Type II is up-down antisymmetric and left-right symmetric (e.g. states 2 and 6). Type III is up-down symmetric and left-right antisymmetric (e.g. states 3 and 7), and Type IV is both up-down and left-right antisymmetric (e.g. state 4). It is well known that antisymmetry can lead to the appearance of nodes in wavefunctions. For example, Type II is up-down antisymmetric, accordingly there occur nodes at $\theta = 0$ and 180°. Since these nodes arise from symmetry constraint, they are called inherent nodes.[13] Types I–IV contain zero, two, two, and four inherent nodes, respectively, and these nodes are unmovable. Incidentally, although states 1 and 5 both belong to Type I without inherent nodes, the latter just contains additional nodes that originate from dynamical excitation. It is found from Fig.3(a) that Ψ_5 has a node at $\theta = \theta_{\rm node} = 51°$. However, due to the up–down symmetry and the left–right symmetry of Type-I state, there must also be nodes occurring at $-\theta_{\rm node}$, $\pi - \theta_{\rm node}$, and $-(\pi - \theta_{\rm node})$. Thus, state 5 contains totally four additional dynamical nodes, which surely implies the occurrence of a strong internal oscillation related to the back-and-forth variation of θ and leads to a much higher energy. Similarly, states 2 and 6 both belong to Type II, but the latter has two inherent nodes together with four additional nodes. In general, the total number of inherent and additional nodes determines the order of levels. Thus, the localized states in the order of increasing energy belong to Type I–IV then again Types I–IV have additional nodes.

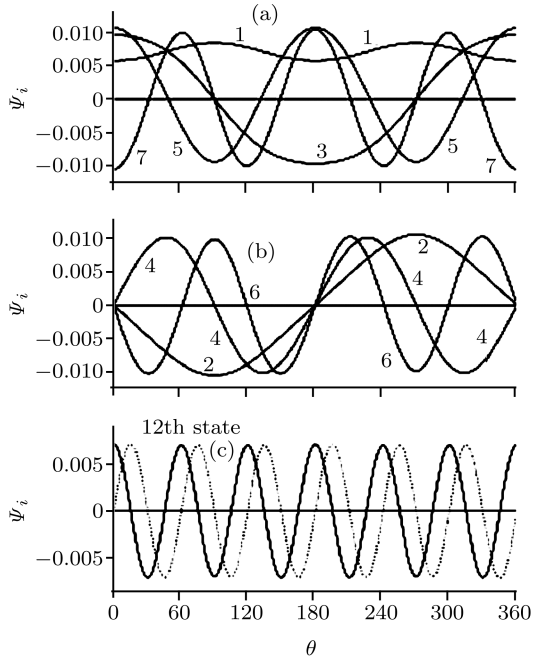


Fig.3. Curves for Ψ_i against θ when $\lambda = \lambda_0$ and $R = 40$ (for the case (C)), where curves are numbered with $i = 1$, 3, 5 and 7 (a), 2, 4 and 6 (b), and 12 (c), and solid and dot lines represent real and imaginary parts of the wavefunctions respectively (the imaginary part appears only in panel (c)).

Furthermore, the (possible) degeneracy of the spectra is discussed. When $R = 0$, the ellipse becomes a circle and the angular momentum is conserved. In

this case most of the states with current $j \neq 0$ should be two-fold degenerate because the state with a clockwise motion ($e^{-ik\theta}$) and its corresponding state with an anti-clockwise motion ($e^{ik\theta}$) have identical energies except for the $k = 0$ state which has $J = 0$. This fact is shown in the left-column of Fig.1 where the degeneracy is clear except for the lowest state. When $R \neq 0$, similarly, there are also two kinds of states. One has $j \neq 0$, which is called non-localized states and has a complex wavefunction. The other one has $J = 0$, which is called localized state and has a pure real or equivalently pure imaginary wavefunction. The first type has exactly the two-fold degeneracy, which is obvious because, if Ψ is a solution, Ψ^* would also be a solution with the same energy. However, the second type does not have this degeneracy, which is simply because $\Psi = \Psi^*$. For the case with $R = 40$, we find that the wavefunctions of the lowest seven states $\Psi_1 - \Psi_7$ are pure real as shown in Fig.3. Accordingly, they have zero current as shown in Fig.2. Thus they are localized states and do not have the exact two-fold degeneracy as shown in the right-column of Fig.1. Nonetheless, some of them are close in energy (e.g. for states Ψ_4 and Ψ_5). Therefore, the spectral lines of these two states are almost overlapped with each other. Incidentally, when $R = 40$, the lowest non-localized states are Ψ_8 and Ψ_9, which are both exactly degenerate.

In general, the density distribution of the localized states is far from uniform. For example, from Fig.3 we know that state 2 is more concentrated at $\theta = \pi/2$ and $3\pi/2$ (upper and lower), while state 3 is more concentrated at $\theta = 0$ and π (left and right, where the curvature is much larger). The difference in spatial distribution leads to a difference in energy. This explains why the energy of Ψ_3 is higher than that of Ψ_2. However, when R is smaller, the effect of the difference in spatial distribution is small. Accordingly, Ψ_3 and Ψ_2 are closer in energy as shown in the middle column of Fig.1. On the other hand, the density of the non-localized states is approximately uniform as shown in Fig.3(c), where the real part and the imaginary part are similar in magnitude, and they match with each other with a constant difference in phase, thereby leading to a steady and strong current.

The total probability of dipole absorption of the Ψ_i state is expressed as $P_i = \sum_f P_{f,i}$ $(E_f > E_i)$ and given in Fig.4. One can see that the more flattened ring has a smaller probability. Besides, there is a fluctuation among the localized states. Now we come to observe the spectra of dipole absorption. The values of absorption probability $P_{f,i}$ of state i ($i = 1, 2$, and 3) against energy $\Delta E = E_f - E_i$ are presented in Fig.5. For the ground state, in case (A) the spectral line of absorption is concentrated at $\Delta E = 7.207$ as shown by the solid line in Fig.5(a), and it is, in fact, a double line related to a transition from state 1 to states 29 and 30 (these two states are degenerate localized states belonging to the excited band). When the ring becomes flattened, these lines split and have a red-shift as shown by the dash and dot lines: a more flattened ring has a larger split and a bigger red-shift. For the higher states, in case (A) there are two and only two spectral lines of absorption (e.g., for the second state, $\Delta E = 7.123$ and 7.280). When the ring becomes flattened, more than two lines of absorption with a larger red-shift may emerge as shown in Figs.5(b) and 5(c).

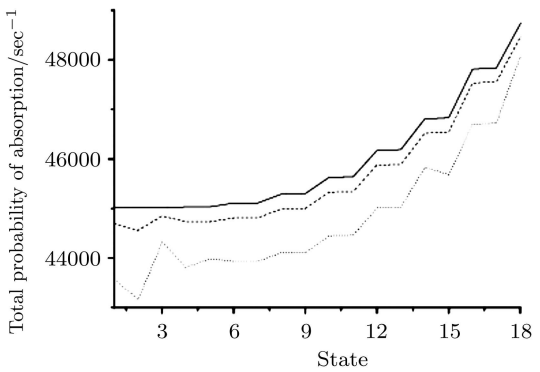


Fig.4. Curves for the values of total probability of absorption P_i against low-lying state, where what solid, dash, and dot lines represent are the same as those in Fig.2.

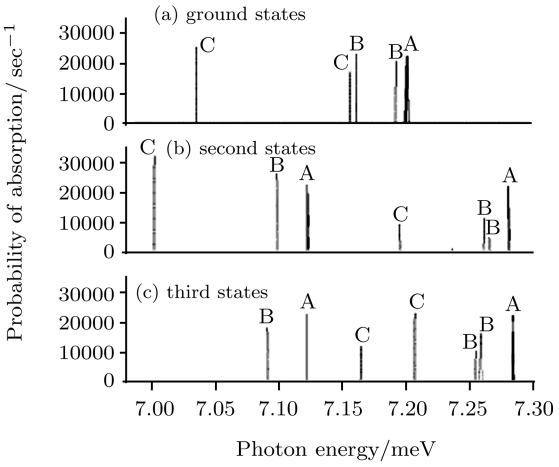


Fig.5. Curves for the values of probability of absorption $P_{f,i}$ of states 1, 2 and 3 in panels (a), (b) and (c), respectively, against the energy $E_f - E_i$ of the photon.

In summary, when a ring becomes flattened, the following points are found.

(i) The higher members of the rotational bands are scarcely affected, while a group of the lowest members of each band are seriously affected, their currents become zero and therefore they become localized.

(ii) There are four types of localized states, i.e. Types I–IV, containing zero, two, two, and four inherent nodes, respectively. In the spectra the localized states are ordered according to their total number of inherent and additional nodes.

(iii) For the localized states, the total probabilities of dipole absorption are small. Their absorption lines each have a remarkable red-shift. In particular, much more than two absorption lines would emerge if the ring is very flattened.

We have studied mainly the effect of the flattening of the ring and found that the optical properties can be adjusted. Another noticeable effect is the one caused by external magnetic field, which is under consideration.

Acknowledgment

The author wishes to thank Professor C. G. Bao and Dr Y. Z. He for helpful discussion.

References

[1] Viefers S, Koskinen P, Singha Deo P and Manninen M 2004 *Physica* E **21** 1
[2] Situ S P 2007 *Commun. Theor. Phys.* **47** 733
[3] Keyser U F, Fuhner C, Borck S, Haug R J, Bichler M, Abstreiter G and Wegscheider W 2003 *Phys. Rev. Lett.* **90** 196601
[4] Mailly D, Chapelier C and Benoit A 1993 *Phys. Rev. Lett.* **70** 2020
[5] Fuhrer A, Luscher S, Ihn T, Heinzel T, Ensslin K, Wegscheider W and Bichler M 2001 *Nature* (London) **413** 822
[6] Hansen A E, Kristensen A, Pedersen S, Sorensen C B and Lindelof P E 2002 *Physica* E (Amsterdam) **12** 770
[7] Van den Broek M and Peeters F M 2001 *Physica* E **11** 345
[8] Lipparini E, Serra L and Puente A 2002 *Eur. Phys. J.* B **27** 409
[9] Even J, Loualiche S and Miska P 2003 *J. Phys.*: *Cond. Matt.* **15** 8737
[10] Yannouleas C and Landman U 2006 *Phys. Status Solidi* A **203** 1160
[11] Berman D, Entin-Wohlman O and Azbel M Ya 1990 *Phys. Rev.* B **42** 9299
[12] Tang A Q 1982 *Quantum Chemistry* (Beijing: Science Press) p49
[13] Bao C G 1992 *Few-Body Systems* **13** 41